PENETROMETRY IN MICROGRAVITY ENVIRONMENTS. Paul Sánchez and Daniel J. Scheeres, Colorado Center for Astrodynamics Research, University of Colorado, Boulder, CO 80309-431 (diego.sanchez-lana@colorado.edu)

Introduction: The use of mechanical devices to sample and penetrate regolith on asteroids is a theme that is gaining the interest for missions of exploration, mitigation and exploitation to these bodies. While there have been many proposals for how such interaction with asteroid regolith can be achieved, the list of missions that have had actual interaction with asteroid surfaces are restricted to the NEAR mission at Eros and the Hayabusa mission at Itokawa. In addition, a new round of asteroid exploration missions are in the final development phases, namely the Hayabusa 2 mission and NASA's OSIRIS-REx mission. A key feature of these missions, and many proposals for future missions, are low energy interactions between the spacecraft and the surface regolith. It is expected that regolith will pool at the geopotential lows on asteroids, and will be prime areas where sampling may occur. Surface accelerations on these bodies and in these regions can be on the order of microgravity, however. The physical interaction between a sampling/landing/anchoring device and the regolith in such environments occurs in conditions that cannot be reconstructed on Earth, and which are very difficult to replicate on-orbit. This makes computer simulations of these interactions a primary tool to evaluate the possible outcomes of these interactions.

Simulation Method: The simulation program we use for this research applies a Soft-Sphere Discrete Element Method [1, 2] to simulate interactions between two types of surface interaction devices. A rigid sampling head that descends into a regolith bed and a right-circular cone shot into the surface of a granular bed. The regolith particles are modeled as spheres that follow a predetermined, but randomized, size distribution and interact through a soft-repulsive potential when in contact. This method considers that two particles are in contact when they overlap. For each particle-particle contact, the code calculates normal and tangential contact forces [3, 1]. Particle-intruder interactions are handled in the same way. The dynamics of the intruders are also driven by their interactions with the regolith.

The calculation of the normal forces between colliding particles is modeled by a linear spring and a dashpot. The elastic force is modelled as

$$\vec{\mathbf{f}}_e = k_n \xi \hat{\mathbf{n}}, \qquad (1)$$

the damping force as:

$$\vec{\mathbf{f}}_d = -\gamma_n \dot{\xi} \hat{\mathbf{n}}, \qquad (2)$$

and the cohesive force (f_c) between the particles is calculated as a function of the size of the particle and the (not simulated) interstitial dust [4].

Then the total normal force is calculated as $\vec{\mathbf{f}}_n = \vec{\mathbf{f}}_e + \vec{\mathbf{f}}_c + \vec{\mathbf{f}}_d$. In these equations k_n is the elastic constant, ξ is the overlap of the particles, γ_n is the damping constant (related to the dashpot), $\dot{\xi}$ is the rate of deformation and $\hat{\mathbf{n}}$ is the vector joining the centres of the colliding particles. This dashpot models the energy dissipation that occurs during a real collision.

The tangential component of the contact force models surface friction, static and dynamic. This is calculated by placing a linear spring at the contact point, attached to both particles, at the beginning of the collision [3, 5], producing a restoring frictional force $\vec{\mathbf{f}}_t$. The magnitude of the elongation of this tangential spring is truncated in order to satisfy the local Coulomb yield criterion $|\vec{\mathbf{f}}_t| \leq \mu |\vec{\mathbf{f}}_n|$. In addition, we have also implemented rolling friction as suggested by [6]. For this, a winding spring provides a torque to particles in contact. In form, it is very similar to surface friction, but is related to the relative angular displacement. This type of friction allows us to obtain aggregates with angles of friction of up to $\sim$35°, typical of cohesionless aggregates on Earth, though angles of $\sim$40° are not rare.

The particles (initially cohesionless and frictionless) are let to settle under Earth's gravity (1g), the same that is slowly decreased until a value of 1 μg is attained. During this process, the particles are also subjected to a velocity and size dependent fluid drag so that the energy stored in the springs can be quickly lost. This methodology [1] results in a porous and weakly coupled regolith.

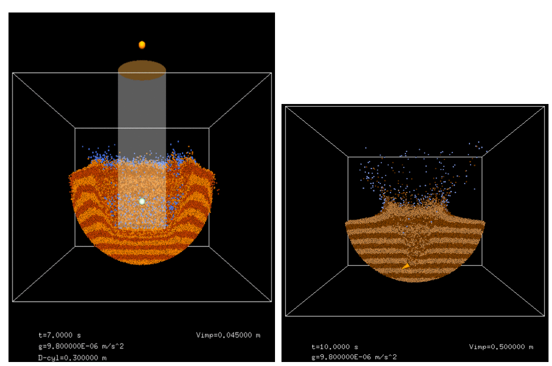

Figure 1: Soft-Sphere DEM simulations with cohesion less regolith; landing pad (left) and cone shot at the granular bed (right).

Regolith and Impactor Models: We assume that the gravitational field is constant and independent of the particle positions, as our study focuses only on a small volume located on the surface on the asteroid. Simulations were carried out with a monodisperse-continuous size distribution (10mm, 20% dispersion).

The landing pad was modeled as an infinite cylinder that could only move vertically. The mass of the cylinder varied to keep a constant surface density on its bottom end as if it were part of a spacecraft of 8000 kg with 3 landing pads(fig. 1 left). The cone was 6 cm high, 3.2 cm in diameter and was modeled as a 6 DOF body (fig. 1 right). For the cylinder, the impact velocity was kept at 4.5 cm/s and regolith cohesion was changed. For the cone, the regolith was left cohesionless, but the impact speed was changed.

Results: Figure 2 shows the position of the bottom end of the cylinder as it penetrates through the regolith. Velocity has been kept at 4.5 cm/s and inter-granular cohesion has been changed from 0 to 3000 Pa. This strength refers to the amount of force that is needed to separate by tension any two grains that were previously in contact, not to the cohesive strength of the aggregate as a whole as is understood in the Druker-Prager yield criterion.

Some of our observations are as follows: 1. the dynamics of the pad do not differ much between pads of different diameters when the grains are cohesionless; 2. cohesive strength always causes greater resistance to penetration; 3. for cohesionless regolith, regardless of the diameter of the pad, the scattered particles have upward velocities of the same order of magnitude as the pad right after impact; 4. cohesion limits the speed of scattered regolith; and 5. cohesive strength of regolith has a significant effect on pad penetration and dynamics

At a “strong Lunar regolith”value of 3000 Pa cohesive strength the pad was completely stopped and rebounded. At a “weak Lunar regolith” value of 100 Pa cohesive strength the pad was stopped in less than 2 seconds. For very low values of cohesion the pad continues to travel for several seconds.

Fig. 3 shows a velocity (v_y) vs. time plot where each line is the average of 5 simulations with the same initial impact velocity, but with a granular bed that has a different random arrangement. Here we have normalized the lines with the impact velocity of the impactor to show the tendency of the behavior and help us find the right fit. For them, we found that the velocity can be fit by:

$$\frac{v_y(t)}{v_i} = \frac{1}{at+b} + c \tag{3}$$

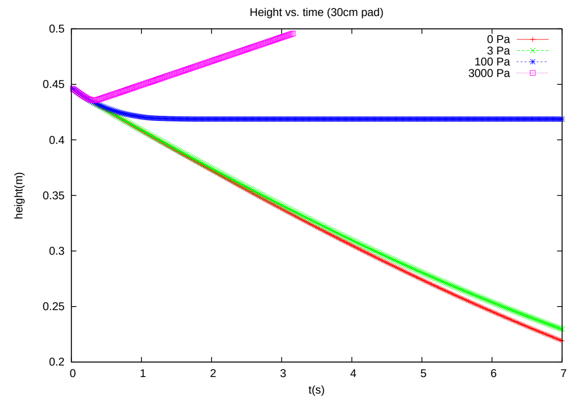

Figure 2: Position of the bottom end of the cylinder as it penetrates through the regolith. Velocity has been kept at 4.5 cm/s and inter-granular cohesion has been changed from 0 to 3000 Pa.

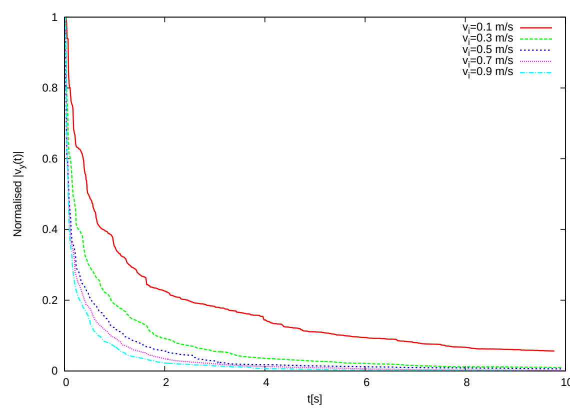

Figure 3: Normalised vertical velocity vs. time plot of the cone after impacts on the granular bed at 0.1 (red), 0.3(green), 0.5 (blue), 0.7 (magenta) and 0.9 (light bue) m/s.

which leads to:

$$a_y(t) = Av_y^2(t) + Bv_y(t) + Cv_i \tag{4}$$

where the quadratic term is the most influential [7].

References: [1] P. Sánchez, et al. (2011) *The Astrophysical Journal* 727(2):120. [2] P. Cundall (1971) in *Proceedings of the International Symposium on Rock Mechanics* vol. 1 129–136 -, Nancy. [3] H. Herrmann, et al. (1998) *Continuum Mechanics and Thermodynamics* 10:189 ISSN 0935-1175 10.1007/s001610050089. [4] P. Sánchez, et al. (2014) *Meteoritics & Planetary Sciences* in press. [5] L. E. Silbert, et al. (2001) *Phys Rev E* 64(5):051302 doi. [6] J. Ai, et al. (2011) *Powder Technology* 206(3):269 ISSN 0032-5910 doi. [7] A. M. Nakamura, et al. (2013) *Icarus* 223(1):222 ISSN 0019-1035 doi.